Migration of a Proton as a Function of Solvation within $\{ROH\}_n\{H_2O\}H^+$ Cluster Ions: Experiment and Theory

Michael M. Y. Lyktey, Robert L. DeLeon, Kevin S. Shores, Thomas R. Furlani, and James F. Garvey*

Department of Chemistry, NSM Complex, State University of New York at Buffalo, Buffalo, New York 14260-3000

Received: March 6, 2000

Metastable and collision-induced decompositions of mass-selected $\{ROH\}_n\{H_2O\}H^+$ cluster ions (where R $\equiv CH_3$–, CH_3CH_2–, $CH_3CH_2CH_2$–, and $(CH_3)_2CH$–) were observed to exhibit distinct size-dependent behavior. We observe that loss of a water molecule is dominant for $n \leq 8$, whereas loss of multiple ROH molecules is the favored decomposition channel for $n \geq 9$, resulting in the eventual formation of a stable $\{ROH\}_9\{H_2O\}H^+$ cluster ion. We believe this is evidence for two distinct cluster geometries which explicitly depend on the number of ROH molecules present. That is, below a certain critical size the proton resides on the molecule with the highest proton affinity, the ROH. However, above that critical cluster size the proton will now preferentially reside on the water molecule, if there are sufficient alcohols to completely and symmetrically solvate the central H_3O^+. The structural implications of these results will be discussed in light of new theoretical calculations which have been performed on this system.

A. Introduction

Molecules which form hydrogen bonds within a gas-phase cluster ion are held together by relatively strong electrostatic forces with average binding energies on the order of 0.5 eV.[1] In recent years, the study of these ion clusters has been conducted with the aim of understanding the effects of hydrogen bonding in solutions and crystals, and the dynamics of solvation-driven reactions following the initial ionization event.[2−17] The reactivity and stability of hydrogen-bonded clusters of various monofunctional compounds have been investigated extensively in neat as well as mixed molecular beam expansions.[2−17] The ionization of neutral hydrogen-bonded clusters, such as water,[3,4] ammonia,[5,18] alcohols,[6,7,19,31,32] and ethers,[20] yield protonated cluster ions via an intracluster ion−molecule reaction.[3]

Cluster ions of the type $\{M\}_n\{H_2O\}_mH^+$, where M has a proton affinity greater than water, have also been the subject of numerous investigations.[20−27,31,32] Studies involving mixed expansions of ethers,[21,22] ketones,[19,22] acetonitrile,[26] and alcohols[28] with water indicate a tendency for the central ion core to change from MH^+ to H_3O^+ at a particular cluster size. A number of molecules which have proton affinities higher than water but are capable of acting only as proton acceptors have exhibited this kind of size-selective proton switch.[19,21,22,26]

Two general pictures of the mixed protonated cluster ion structures have emerged from the work to date: one in which the alcohols and waters form a linear hydrogen-bonded chain, and one in which the alcohols and waters are hydrogen-bonded cyclically. Because the structure of such a cluster ion is difficult to prove experimentally, it has been a topic of considerable debate. Another related source of disagreement is the association of the proton in mixed cluster ions. While it is generally agreed that for the smallest clusters the alcohols are most closely associated with the proton due to greater proton affinity compared to water, this association is uncertain in larger clusters.

Recently, Chang and co-workers[29] have reported the observation that within a cluster a proton can migrate from solute to solvent molecules upon asymmetetric solvation. These workers showed spectroscopic data indicating that, in the case of cluster ions of the type $\{H_2O\}_n\{(CH_3)_2O\}H^+$, for $n = 1$ the proton sits on the ether and it is equally shared by both molecules at $n = 2$, but for $n > 2$ it will instead sit on a water. In contrast, on the basis of mass spectrometric magic numbers, we had previously suggested just the opposite for the case of $\{ROH\}_n\{H_2O\}H^+$ cluster ions.[30] That is, this system was an example where the proton shifts from solvent to solute when there are enough solvent molecules to symmetrically solvate the core H_3O^+ cation. In that paper we suggested a structure for the most intense mass peak observed, $\{ROH\}_9\{H_2O\}H^+$, and a theoretical calculation of that structure is depicted in Figure 1. This

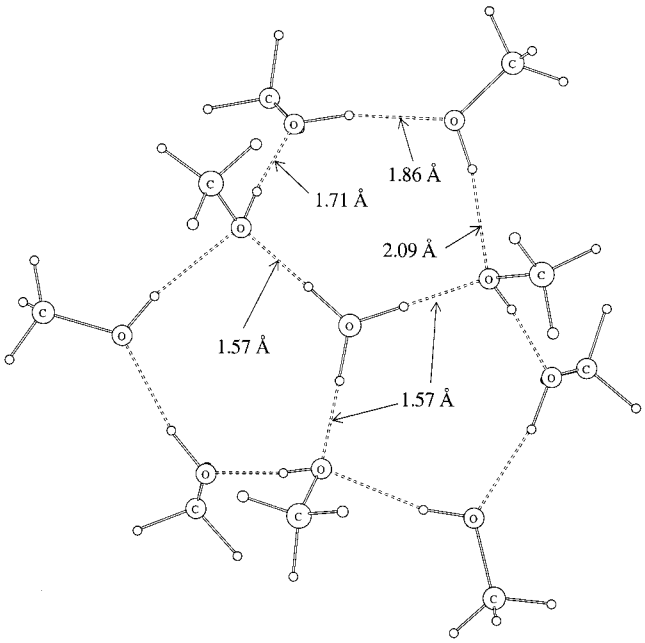

Figure 1. Optimized structure for the magic number cluster $\{CH_3OH\}_9\{H_3O\}^+$. Details of the calculation are presented in the text.

10.1021/jp000872n CCC: $19.00
Published on Web 05/16/2000

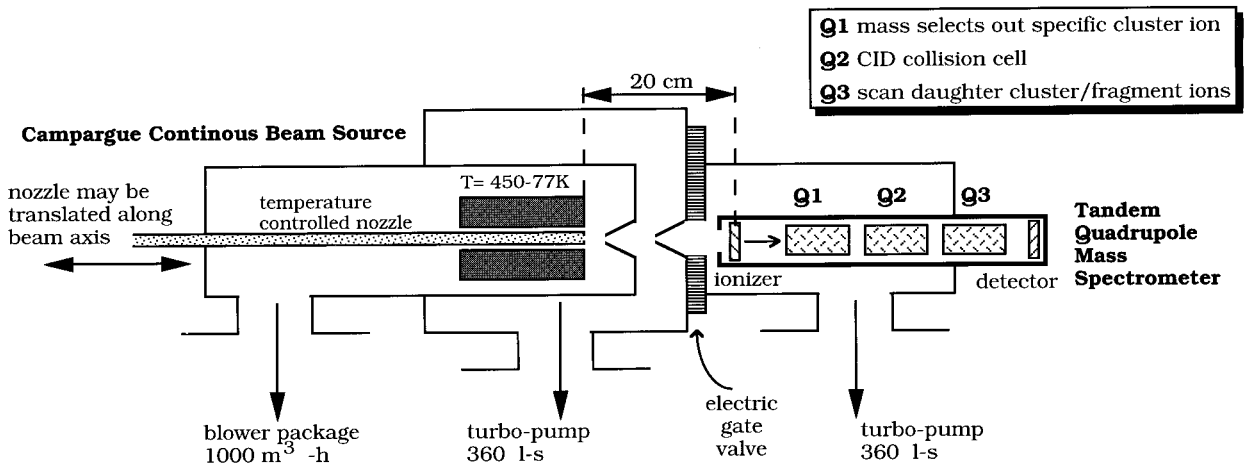

Figure 2. Schematic of the apparatus.

particular structure maximizes the number of hydrogen bonds possible and completely solvates the core H_3O^+ cation with the nine methanols. Karpas and co-workers have employed tandem mass spectrometry to study these $\{ROH\}_n\{H_2O\}H^+$ ions. Through mass selecting a specific cluster ion and employing collision-induced dissociation (CID), they observed only water loss for $n \leq 7$ for methanol[31] and ethanol, propanol, and butanol.

$$\{ROH\}_n\{H_2O\}H^+ \rightarrow \{ROH\}_nH^+ + H_2O \qquad n \rightarrow 7 \qquad (1)$$

They suggested that these results were consistent with the proton sitting on the alcohol. The proposed structure of the cluster ion would then be a chain of hydrogen-bonded solvent molecules with the water only weakly held to the cluster ion. However, for the particular case of methanol, for $n \geq 9$, a 50:50 loss of either a water or a methanol was observed. It is important to note that in this set of experiments the cluster ions were generated from an atmospheric pressure ionization source (API), where the clusters are generated in a high-pressure corona. As these ions are extracted, changes in both cluster composition and structure can occur. Different cluster ion structures, which are not equilibrated, may result such that using this technique it is not possible to reproduce previously reported magic numbers as seen in molecular beam experiments.[30] The CID collision cell pressures employed[31,32] were also high enough to cause complete decomposition of the parent ions, in contrast to the experiments which will be described below.

In this paper, we present results of our tandem mass spectrometric investigations of $\{ROH\}_n\{H_2O\}H^+$ cluster ions, where R $\equiv$ CH_3–, CH_3CH_2–, $CH_3CH_2CH_2$–, and $(CH_3)_2CH$–. We first generate large neutral heteroclusters of the type $\{ROH\}_x\{H_2O\}_y$ via an intense molecular beam expansion. Following formation and skimming, a small fraction of these neutral clusters are subsequently ionized via electron impact and then mass-selected. In the microseconds following the ionization process, but prior to actual mass selection, the resulting $\{ROH\}_n\{H_2O\}_mH^+$ cluster ions undergo extensive evaporation as the cluster ion cools and eventually adopts a stable structure. Like Karpas and co-workers, we too observe that, for CID of $\{ROH\}_{n\leq7}\{H_2O\}H^+$ cluster ions, water loss dominates independent of alcohol type. However, in contrast to Karpas and co-workers, we now also observe that, for CID of $\{ROH\}_{n\geq8}\{H_2O\}H^+$ cluster ions, ROH loss dominates, again independent of the alcohol type. Following collisional activation, we see successive ROH loss in the same cluster, which, given enough excess energy, eventually evaporates down to the magic number cluster ion, $\{ROH\}_9\{H_2O\}H^+$. This particular process is summarized in the following equation:

$$\{ROH\}_n\{H_2O\}H^+ \rightarrow \{ROH\}_9\{H_2O\}H^+ + (n-9)ROH \qquad (2)$$

Lastly, due to the intense cluster beam generated in the present study we are also able to directly observe metastable decomposition in $\{ROH\}_n\{H_2O\}H^+$. This is in contrast to typical CID processes where the cluster ion is energized via inelastic collisions with a bath gas, leading then to further evaporation and even fragmentation. For our metastable studies we can evacuate the collision cell and observe spontaneous evaporation from the small fraction of cluster ions which still possess sufficient excess energy to lose additional monomers. In this case we typically observe only loss of a single molecule from the cluster ion, and once again see for $n < 7$ only loss of a single water and for $n > 9$ only loss of a single methanol. We note that the metastable decomposition is a much more sensitive probe of structure and is far more selective in product formation.

To summarize, we will present in this paper molecular beam/tandem mass spectrometeic results which support two conclusions: (1) The site of protonation within the cluster shifts from a water to an alcohol as a direct function of cluster size, for cluster ions of the type $\{ROH\}_n\{H_2O\}H^+$. This result is independent of the type of alcohol employed. (2) Evidence for the enhanced stability of the cluster ion $\{ROH\}_9\{H_2O\}H^+$ suggests a stable structure. We believe that this work illustrates the utility of employing tandem mass spectrometry with molecular beams to study geometric effects within cluster ions.[33–35]

B. Experiment

The apparatus used in this study consists of a continuous molecular beam source coupled to a triple quadrupole mass spectrometer as shown in Figure 2. Neutral clusters are generated using a Campargue-type beam source[36] with a 250 μm nozzle diameter at a distance of 5.0 mm from a conical skimmer. The neutral cluster beam is skimmed and collimated by a second skimmer before entering the chamber containing the tandem mass spectrometer system. A small fraction of this neutral cluster beam is ionized by a collinear electron impact ionizer, and the ions are accelerated into the first quadrupole mass filter of the triple quadrupole mass spectrometer. The electron energy in this study was varied in the range 20.0−100.0 eV, while the emission

TABLE 1: Metastable Decay Channels for $\{ROH\}_n\{H_2O\}H^+$ Species[a]

	M_nWH^+			E_nWH^+			P_nWH^+			Q_nWH^+		
n	−W	−M	−W and −M	−W	−E	−W and −E	−W	−P	−W and −P	−W	−Q	−W and −Q
3	100	0	0	100	0	0	100	0	0	100	0	0
4	100	0	0	100	0	0	100	0	0	100	0	0
5	100	0	0	100	0	0	100	0	0	100	0	0
6	100	0	0	89.6	4.7	5.7	100	0	0	100	0	0
7	87.3	2.2	10.5	97.0	1.3	1.7	100	0	0	96.8	0	3.2
8	78.4	18.8	2.8	84.9	11.1	4.0	100	0	0	86.9	13.1	0
9	2.7	97.3	0	29.2	61.2	9.6	66.5	24.3	9.2	10.7	89.3	0
10	0	100	0	4.5	84.8	10.7	36.4	53.5	10.1	0	100	0
11	0	100	0	0	100	0	23.3	76.7	0	0	100	0
12	0	100	0	0	100	0	17.1	82.9	0	0	100	0

[a] Daughter ion intensities as a percentage of the total daughter ion signal observed in the metastable decay mass spectra for the series $\{ROH\}_n\{H_2O\}H^+$, where ROH is methanol (M), ethanol (E), 1-propanol (P), or 2-propanol (Q). In each case, a 13% mixture of water (W) in alcohol (v/v) seeded in helium was used at a total stagnation pressure of 3.0 atm. The resulting gas mixture was expanded through a 250 μm Campargue-type nozzle at 278 K, and the resulting cluster beam was ionized by electron impact at an ionization energy of 30.0 eV. The pressure in the collision cell (Q2) ranged from 1.0×10^{-6} to 2.2×10^{-6} Torr.

current was held constant at 1.00 mA. It was found that variations of the electron energy tend to either increase or decrease the entire spectrum without any major shifts in the relative sizes of the various peaks. The triple quadrupole used in this study is commercially available (Extrel Co.) and designed for use in molecular beam sources. The first (Q1) and third (Q3) quadrupoles can be operated in either an "rf-only" or a mass scan mode. Both mass analyzers have a nominal mass range of 1200 amu. The second quadrupole (Q2) contains the collision cell and is always operated in the rf-only mode that will transmit ions with a wide range of *m*/*z* ratios. The MS/MS spectra were obtained by first mass selecting a particular cluster ion with Q1. The products of metastable and collision-induced decompositions were mass-analyzed using Q3. The laboratory frame collision energy is determined by the difference in the effective source potential and the dc level of the second quadrupole.

C. Results

1. Metastable Decay Mass Spectra. The metastable decay processes of individual cluster ions were studied in the MS/MS mode. Decompositions of selected ions of the type $\{ROH\}_n\{H_2O\}H^+$ were examined for ROH = methanol, ethanol, 1-propanol, and 2-propanol. The results of these studies are summarized in Table 1. The product ions are normalized to the percentage of all observed product ions.

Aside from the identity of the alcohol, the parameters for the acquisition of these spectra were identical. Alcohol and water were seeded in helium by bubbling the gas through a 13% solution (v/v) of distilled water in alcohol at a total stagnation pressure of 3.0 atm. The gas mixture was expanded through the 250 μm orifice of a Campargue-type nozzle at 278 K, and the resulting cluster beam was ionized by electron impact at an ionization energy of 30.0 eV. The parent ion of interest was mass-selected in quadrupole 1 (Q1). It then passed into the evacuated collision cell (Q2) with a lab frame ion energy of 100 eV, where the pressure was between 1.0×10^{-6} and 2.2×10^{-6} Torr. Because the collisional cross-sections of these cluster ions are not known, and only relative cross-sections may be calculated from the present data, it is uncertain exactly *how* many collisions the ions undergo in Q2. However, given that the residence times of the ions in Q2 are all on the order of 10^{-5} s and using conservative approximations of collisional cross-sections, it is estimated that the average ion experiences less than a single collision in the collision cell.

The metatstable spectra were indeed very simple to interpret and quite definitive. Only three unimolecular decomposition channels were observed for a given $\{ROH\}_n\{H_2O\}H^+$ series: loss of H_2O, loss of ROH, or loss of ROH + H_2O. In all cases, except for the 1-propanol/water system where the transition is more gradual, we note that there is a dramatic change in preference from loss of H_2O to loss of ROH between $n = 8$ and $n = 9$. That is, for $n \leq 7$ only water loss is observed independent of how many alcohols are present. For $n > 10$ only the loss of a single alcohol is now observed.

2. Collision-Induced Dissociation Mass Spectra. The CID of individual $\{ROH\}_n\{H_2O\}H^+$ ions was also investigated for ROH = methanol, ethanol, 1-propanol, and 2-propanol in the MS/MS mode. Typical CID spectra for the methanol/water system are shown in Figure 3. The plotted results of these studies for the entire set of alcohols are shown in Figures 4−7. The conditions under which the CID mass spectra were acquired are very similar to those employed for the metastable decay mass spectra given above. The only difference was that helium was introduced into the collision cell as a collision gas in the present case, so that the total pressure in the collision cell was between 8.0×10^{-4} and 1.0×10^{-3} Torr. A center-of-mass collision energy of 0.5 eV was used in all cases; however, general results were not observed to differ substantially when constant lab frame collision energy was used. As discussed in the previous section, it is difficult to determine accurately the average number of collisions experienced by a given cluster ion with a 100 eV lab frame collision energy. However, rough estimates indicate that under these conditions a cluster ion will certainly undergo multiple collisions.

For each alcohol/water system, more extensive dissociation channels are observed in comparison to those seen in the metastable decay mass spectra. Figure 3 shows typical data for cluster ions of the type $\{CH_3OH\}_n\{H_2O\}H^+$ where $n = 6$, 9, and 12. We observe that the changes in preference from loss of H_2O to loss of ROH still occur between $n = 8$ and $n = 9$ for all alcohols, except 1-propanol, where the "crossover" is observed between $n = 9$ and $n = 10$. At lower *n* values, the loss of H_2O and loss of ROH + H_2O channels are dominant, whereas at the highest *n* values the loss of ROH and loss of multiple ROH molecules dominate.

D. Discussion

The results of our present study are in agreement with a recent investigation involving $\{HCOOH\}_n\{H_2O\}H^+$ cluster ions, where the loss of water was reported to be the favored channel for $n = 1-3$, whereas cluster ions with $n \geq 4$ preferentially lost formic acid.[37] These results were also rationalized by suggesting

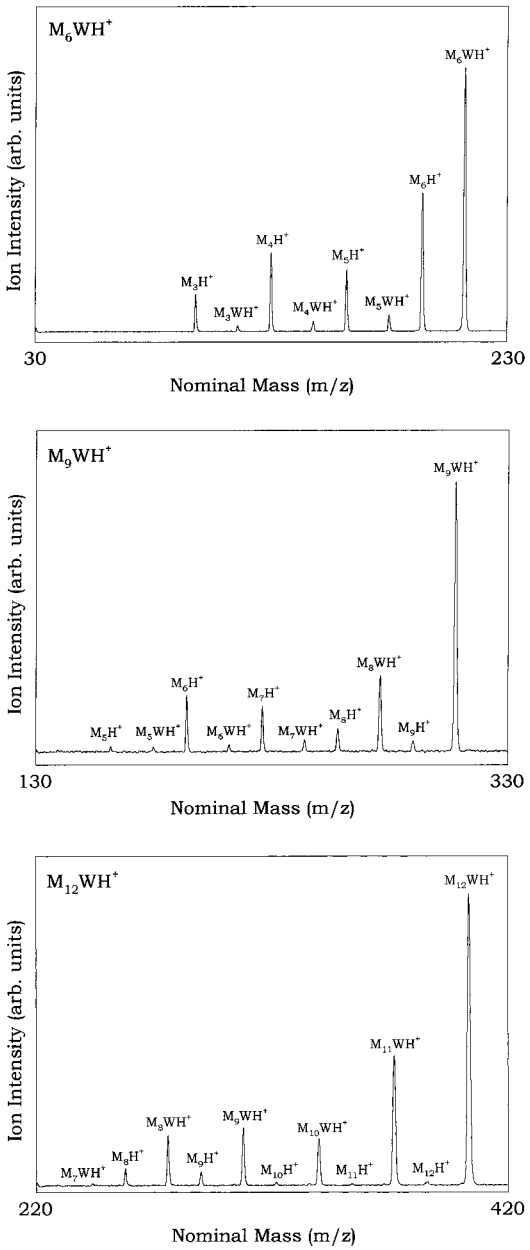

Figure 3. CID spectra for (a, top) $\{CH_3O\}_6\{H_2O\}H^+$, (b, middle) $\{CH_3OH\}_9\{H_2O\}H^+$; and (c, top) $\{CH_3OH\}_{12}\{H_2O\}H^+$. The translational energy of these ions was set to 10.0 eV (lab) and the pressure in the collision cell region was $(9.0 \pm 1.0) \times 10^{-4}$ Torr.

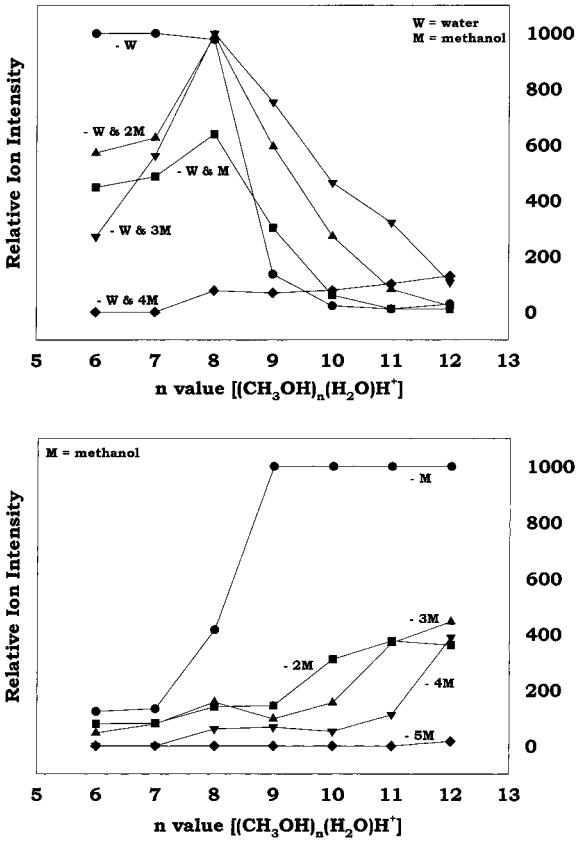

Figure 4. CID loss channels for $\{CH_3OH\}_n\{H_2O\}H^+$ cluster ions as a function of *n*. (a, top) represents water loss channels, while (b, bottom) represents alcohol loss channels.

that small cluster ions form stable open chain structures with the water molecule located in the periphery of the cluster ion and above a critical cluster size the stable structures have a central hydronium ion solvated extensively by a ring of formic acid molecules. The results of the study involving $\{HCOOH\}_n\{H_2O\}H^+$ were stated to be in agreement with the experimental and theoretical studies of protonated acetic acid/water clusters.

The fused cyclic or half-clathrate structure for $\{ROH\}_9\{H_2O\}H^+$ cluster ions was proposed by Garvey and co-workers primarily on the basis of the observation of "magic numbers" in the cluster mass spectra.[30] The idea behind this model is that, at $n = 9$, the proton goes from being associated with the alcohol to being incorporated into a fully solvated hydronium ion, H_3O^+. Despite H_2O having a lower proton affinity than any of the alcohols, this structure was proposed to be more stable than the linear arrangement because it enables the most extensive hydrogen-bonding network to be formed. We note that a previous study[38] of water and alcohol clusters concluded that clathrate structures exhibited enhanced stability in mixed water−methanol cluster ions.

To explore this possibility, a geometry optimization was carried out on the magic number cluster $\{CH_3OH\}_9\{H_3O\}^+$, using the computational chemistry program Gaussian94.[39] The geometry optimization was carried out at the Hartree−Fock level using a standard 6-31G(d,p) basis set. In the initial guess structure, the H_3O^+ cation was placed at the center of the methanol cluster to maximize the number of available hydrogen bonds. Since the solvation shell is complete, there are no unbonded hydrogen-bonded hydrogens (so-called "dangling hydrogens"), making the hydrogen-bonding extremely efficient. This "efficiency" is evident in the optimized structure which is shown in Figure 1. Note that all nine of the methanol oxygens are hydrogen-bonded to the hydrogen of an adjacent methanol group, and that all three hydrogens of H_3O^+ are involved in hydrogen bond formation (with three of the nine methanol oxygens). The final optimized structure is strikingly symmetric. The hydrogen bonds to the central H_3O^+ are all 1.57 Å, while the hydrogen bonds in the outer ring alternate among 1.71, 1.86, and 2.09 Å (as indicated in the figure). In terms of energetics, the optimized structure shown in Figure 1 was found to be about 38 kJ/mol more stable than a structure proposed by Karpas[31] in which the H_3O^+ is hydrogen-bonded to the end of a linear chain of hydrogen-bonded methanols (−1111.970 04 hartrees versus −1111.955 62 hartrees, HF theory, 6-31G(d,p) basis). It is interesing to also note that our proposed cyclic structure is about 14 kJ/mol lower in energy than the linear hydrogen-bonded methanol chain structure, also proposed by Karpas,[31] with a H_3O^+ now in the center (−1111.970 04 hartrees versus −1111.964 70 hartrees using HF theory and a 6-31G(d,p) basis).

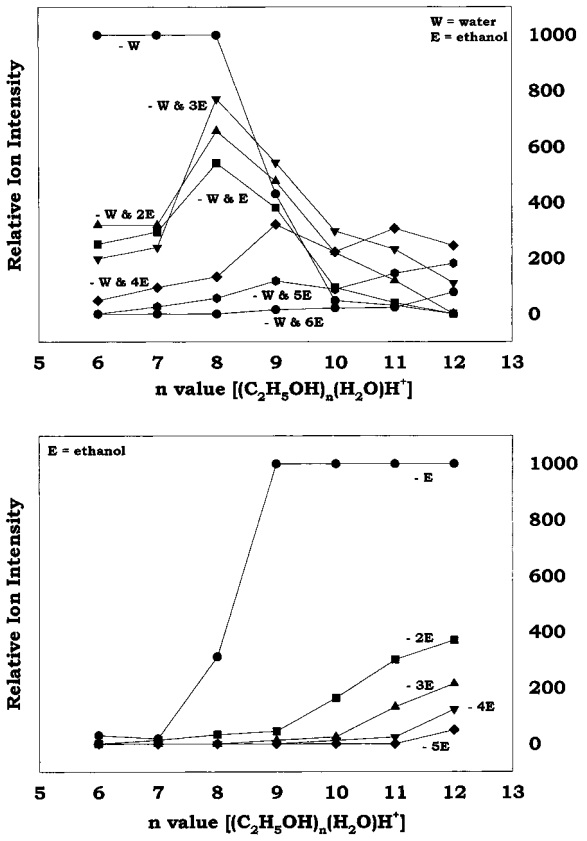

Figure 5. CID loss channels for $\{CH_3CH_2OH\}_n\{H_2O\}H^+$ cluster ions as a function of *n*. (a, top) represents water loss channels, while (b, bottom) represents alcohol loss channels.

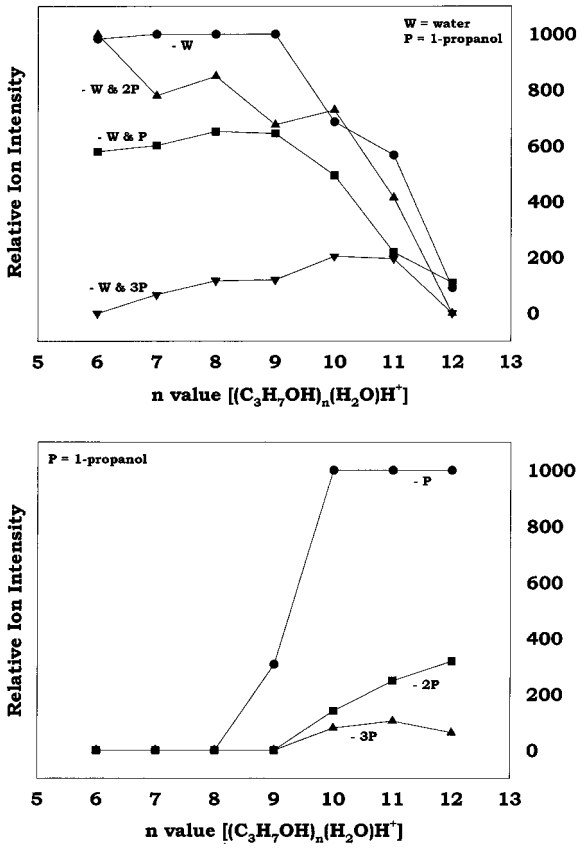

Figure 6. CID loss channels for $\{CH_3CH_2CH_2OH\}_n\{H_2O\}H^+$ cluster ions as a function of *n*. (a, top) represents water loss channels, while (b, bottom) represents alcohol loss channels.

On the basis of the structure shown in Figure 1, one would predict that loss of a methanol group, which involves the rupture of only two relatively weak hydrogen bonds, would be energetically favored over loss of H_2O, which involves the breaking of a chemical bond (OH) in addition to two hydrogen bonds. While the loss of methanol is indeed energetically favored, calculations described below indicate that loss of H_2O does not require anywhere near the energy associated with breaking a covalent bond. This is because all three hydrogens of the central H_3O are relatively free to move between the oxygen of the H_3O and the oxygen of the corresponding methanol group. Figure 8 shows the energy profile, carried out using both Hartree−Fock and density functional theory (6-31G(d,p) basis set), for the movement of a hydrogen between the oxygen of the central water molecule and the methanol oxygen to which it is hydrogen-bonded. In each case the profile was generated using the Gaussian94 SCAN function in which all degrees of freedom other than the O−H−O distance are held fixed. For both levels of theory, a single minimum occurs when the hydrogen is about 1 Å from the central oxygen (of H_3O). Somewhat surprisingly, neither theory predicts that a minimum exists on the methanol side. From Figure 8, migration of a H_3O *hydrogen* from its equilibrium position (1.0 Å from the central oxygen atom) to a position that is about 1 Å away from the methanol oxygen (a move of about 0.5 Å) requires about 42 kJ/mol in energy. Thus, loss of H_2O from the structure shown in Figure 1 would require not only the rupture of two strong hydrogen bonds (as indicated by the relatively short hydrogen bond length of 1.57 Å) *but also an additional 42 kJ/ mol for the H left behind to migrate to the methanol oxygen* (as indicated by the energy profile shown in Figure 8). However, loss of methanol from the cluster requires only the rupture of two relatively weak hydrogen bonds (1.86 and 2.09 Å; see Figure 1). We therefore estimate that loss of water from the cluster requires *at least 42 kJ/ mol more energy* than does loss of methanol. The actual energy difference is probably considerably larger given the shorter (stronger) hydrogen bonds of the central H_3O as compared to the longer (weaker) hydrogen bonds of the outer methanols.

While hydrogen bonding is an important factor in the stability of the fused cyclic structure, it is not the strength of the individual bonds, but the number of bonds which are formed, that is significant. As all of the alcohol/water systems form the same number of hydrogen bonds in the half-clathrate structure, hydrogen bonding will be a minor consideration in explaining the differences among the five systems. The proton affinities of the alcohols and water, and the "size" of the alkyl groups involved will probably be the parameters most responsible for the differences among the various alcohol systems. Steric hindrance will likely be a key factor since the alcohols are in a very orderly arrangement around the central H_3O^+, and as such, the alkyl groups of the alcohols may be forced into positions where they sterically interact with one another. This may account for the qualitative difference we observe for the two propanols. The proton affinities may be important if the difference between that of water and that of one of the alcohols is extremely large. In this case, the difference may actually become too great to be overcome by the added stability of increased hydrogen bonding. In our case the proton affinity of water is 727 kJ/mol, while those of the alcohols are as follows: methanol, 777 kJ/mol; ethanol, 799 kJ/mol; 1-propanol, 804 kJ/mol; 2-propanol, 816 kJ/mol.[40] On the basis of these numbers, one would expect that, for cluster ions of the type $\{ROH\}_n\{H_2O\}H^+$, the proton would always reside on the alcohol, which is the better base. For the proton to shift to the water at larger cluster sizes, one must argue

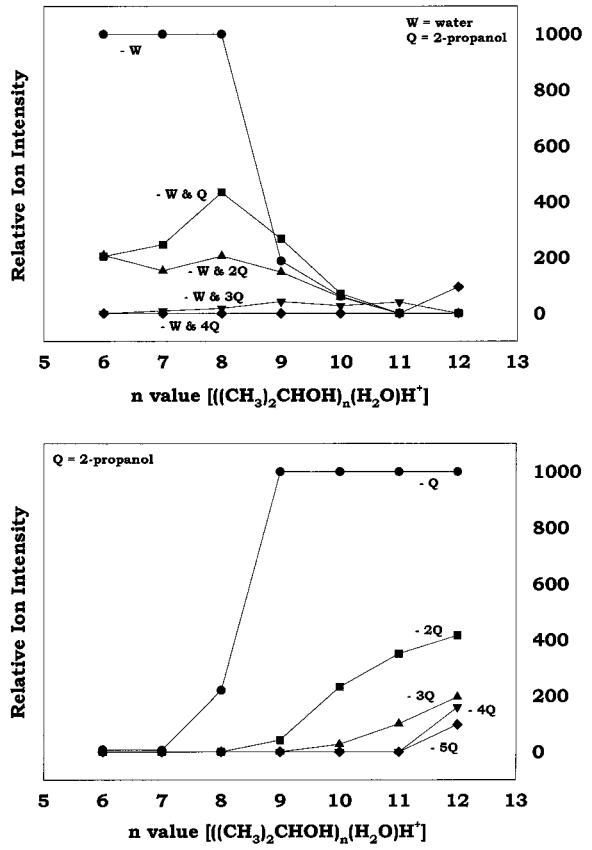

Figure 7. CID loss channels for $\{(CH_3)_2CHOH\}_n\{H_2O\}H^+$ cluster ions as a function of *n*. (a, top) represents water loss channels, while (b, bottom) represents alcohol loss channels.

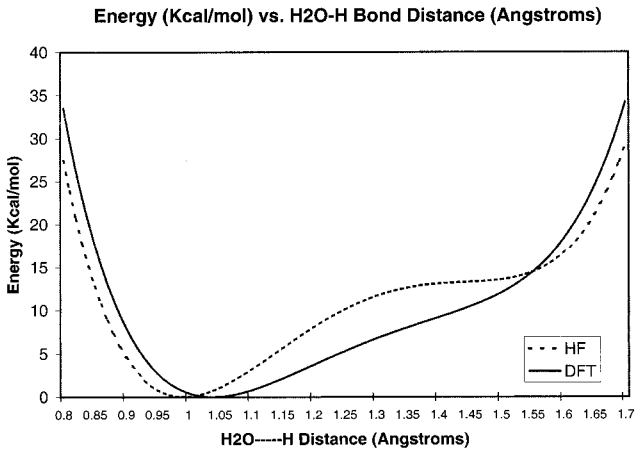

Figure 8. Energy versus H_2O-H distance computed at both the Hartree−Fock and DFT levels employing a 6-31G(d,p) basis set. The distance between the oxygen on the water and the oxygen on the methanol is fixed at 2.567 Å, such that a H_2O-H distance of 1.57 Å corresponds to a $H-OHCH_3$ distance of 1.0 Å.

that there must be a favorable energetic reason for the switch, on the basis of geometric considerations (Figure 1). In spite of the unfavorable ionization potential difference between methanol and water, experimental evidence for the existence of H_3O^+ in water/alcohol mixtures has also been recently reported.[41] In that study of cluster ions of the type $\{CH_3OH\}_1\{H_2O\}_{1-6}H^+$ it was concluded that the proton could reside on either the methanol or the water molecule.

Considering the above factors, the changes in solvent preference are very consistent with the half-clathrate structure. Using the best estimates of bond lengths, bond angles, and hydrogen bond "lengths" available for water and the alcohols, the half-clathrate structure was modeled as a function of the size of the alkyl group.[42] We observed that the only alkyl group capable of direct steric interaction with an adjacent alkyl group of the same type was the 1-propyl group. On this basis, it is proposed that when ROH is methanol, ethanol, or 2-propanol for the $\{ROH\}_n\{H_2O\}H^+$ series, a fused cyclic structure is formed at $n = 9$. When ROH is 1-propanol, however, any five-membered cyclic structure introduces steric hindrance, and so $(C_3H_7OH)_9(H_2O)H^+$ may likely possess a different structure. So while the changes in preference from loss of H_2O to loss of ROH all take place between $n = 8$ and $n = 9$ for ROH = methanol, ethanol, and 2-propanol, it is not surprising that 1-propanol should exhibit different behavior.

The fused cyclic model agrees with the detailed features in the methanol, ethanol, and 2-propanol, and methanol/2-propanol MS/MS spectra, as well. The observations that loss of ROH is dominant over all other channels at $n = 10$, loss of two CH_3OH or C_2H_5OH molecules is the only secondary channel at $n = 11$, and loss of three CH_3OH or C_2H_5OH molecules grows in at $n = 12$ are consistent with the fact that any ROH molecules beyond $n = 9$ are very loosely bound in this structure (no data are available at $n \geq 10$ for 2-propanol, since the parent ions were too weak). In each case, the cluster ion tends to lose as many alcohols as necessary to reach the $\{ROH\}_9\{H_2O\}H^+$ configuration. The dramatic decrease in loss of H_2O is expected since the proton is now associated with H_2O in this structure, and the H_3O^+ is proposed to be the central ion. Therefore, loss of H_2O would require excessive energy, since three hydrogen bonds would need to be broken.

E. Conclusions

We have studied mixed expansions of various alcohols with water via molecular beam/tandem mass spectrometry. By mass selecting cluster ions of type $\{ROH\}_n\{H_2O\}H^+$, we have been able to probe their structural differences as a function of their stoichiometry, through both collision-induced dissociation and, more sensitively, metastable decomposition.

From Table 1, it can be observed that the loss of a single water molecule is the dominant metastable decomposition channel in $\{ROH\}_n\{H_2O\}H^+$ heterocluster ions with $n = 2 - 8$. This indicates that the proton is associated with the ROH molecule, which indeed possesses the higher proton affinity. It is also consistent with a structural model where the ROH molecules form a chainlike structure with the water molecule relegated to the end of the hydrogen-bonded chain, such that the loss of a water molecule would be more facile. However, in the heterocluster ions with $n \geq 8$ it is loss of the ROH molecule which becomes the dominant metastable decomposition channel. These data support our earlier speculation[30] that the preferred retention of water in $\{ROH\}_n\{H_2O\}H^+$ for $n \geq 8$ is indicative of a switch in the location of the proton from the alcohol to the water molecule. That is, in larger clusters ($n \geq 8$) the central hydronium ion is completely solvated by a ring of hydrogen-bonded alcohol molecules. The loss of only a single ROH molecule from $\{ROH\}_n\{H_2O\}H^+$ cluster ions with $n \geq 9$ is consistent with the completion of the first solvation shell at $n = 9$. Heterocluster ions with greater than nine ROH molecules would have the ROH molecules located in the second solvation shell and, hence, would be bound more weakly and be lost with greater ease. This result is also borne out in the CID studies which we report in this paper as well as by previous work by Karpas and co-workers.[31,32] Indeed in our CID study for clusters of the type $\{ROH\}_{n>9}\{H_2O\}H^+$ we show multiple

ROH loss for the cluster to generate a cluster ion with a stoichiometry of $\{ROH\}_9\{H_2O\}H^+$. This again we believe to be evidence of alcohols from the secondary solvation shell evaporating away to leave behind the stable cluster ion as shown in Figure 1.

Acknowledgment. J.F.G. and T.R.F. acknowledge support from NSF Grant ATM971338. T.R.F. also acknowledges additional support from NSF Grants DBI9871132 and NIH Grant GM58295-01. Access to the Origin2000 at the State University of New York at Buffalo's Center for Computational Research is also greatly appreciated. We also thank Mr. Michael Hall for aid with the Spartan calculations.

References and Notes

(1) Jortner, J. *Ber. Bunsen-Ges. Phys. Chem*. **1984**, *88*, 188.
(2) Curtiss, L. A.; Blander, M. *Chem. Rev*. **1988**, *88*, 827.
(3) Klots, C. E.; Compton, R. N. *J. Chem. Phys*. **1978**, *69*, 1636.
(4) Herman, V.; Kay, B. D.; Castleman, A. W., Jr. *J. Chem. Phys*. **1982**, *72*, 185.
(5) Echt, O.; Morgan, S.; Dao, P. D.; Stanley, R. J.; Castleman, A.W., Jr. *Ber. Bunsen-Ges. Phys. Chem*. **1984**, *88*, 217.
(6) Morgan, S.; Castleman, A. W., Jr. *J. Am. Chem. Soc*. **1987**, *109*, 2867.
(7) Shukla, A. K.; Stace, A. J. *J. Phys. Chem*. **1988**, *92*, 2579.
(8) Garvey, J. F.; Bernstein, R. B. *J. Am. Chem. Soc*. **1986**, *106*, 6096.
(9) Garvey, J. F.; Bernstein, R. B. *J. Am. Chem. Soc*. **1987**, *109*, 1921.
(10) Morgan, S.; Keesee, R. G.; Castleman, A. W., Jr. *J. Am. Chem. Soc*. **1989**, *111*, 3841.
(11) Morgan, S.; Castleman, A. W., Jr. *J. Phys. Chem*. **1989**, *93*, 4544.
(12) Tzeng, W. B.; Wei, S.; Castleman, A. W., Jr. *Chem. Phys. Lett*. **1990**, *166*, 343.
(13) Tzeng, W. B.; Wei, S.; Castleman, A. W., Jr. *Chem. Phys. Lett*. **1990**, *168*, 30.
(14) Wei, S.; Tzeng, W. B.; Castleman, A. W., Jr. *J. Phys. Chem*. **1991**, *95*, 585.
(15) Wei, S.; Tzeng, W. B.; Castleman, A. W., Jr. *J. Phys. Chem*. **1990**, *94*, 6927.
(16) Meot-Ner, M.; Speller, C. V. *J. Phys. Chem*. **1989**, *93*, 3663.
(17) Mestdagh, J. M.; Binet, A.; Sublemontier, O. *J. Phys. Chem*. **1989**, *93*, 8300.
(18) Peifer, W. R.; Coolbaugh, M. T.; Garvey, J. F. *J. Chem. Phys*. **1989**, *91*, 6684.
(19) (a) Herron, W. J.; Coolbaugh, M. T.; Vaidyanathan, G.; Garvey, J. F. *J. Am. Chem. Soc*. **1990**, *114*, 3684. (b) Xia, P.; Hall, M; Fulani, T. R.; Garvey, J. F. *J. Phys. Chem*. **1996**, *100*, 12235.
(20) Coolbaugh, M. T.; Peifer, W. R.; Garvey, J. F. *J. Am. Chem. Soc*. **1990**, *112*, 3692.
(21) Wei, S.; Tzeng, W. B.; Castleman, A. W., Jr. *J. Phys. Chem*. **1991**, *95*, 5080.
(22) Stace, A. J., Moore, C. *J. Phys. Chem*. **1982**, *86*, 3681.
(23) Kebarle, P.; Haynes, R. N.; Collins, J. G. *J. Am. Chem. Soc*. **1967**, *89*, 5753.
(24) Stace, A. J.; Shukla, A. K. *J. Am. Chem. Soc*. **1982**, *104*, 5314.
(25) Stace, A. J.; Moore, C. *J. Am. Chem. Soc*. **1983**, *105*, 1814.
(26) Deakyne, C. A.; Meot-Ner, M.; Campbell, C. L.; Hughes, M. G.; Murphy, S. P. *J. Am. Chem. Soc*. **1986**, *84*, 4958.
(27) Wei, S.; Tzeng, W. B.; Keesee, R. G.; Castleman, A. W., Jr. *J. Am. Chem. Soc*. **1991**, *113*, 1960.
(28) (a) Garvey, J. F.; Herron, W. J.; Vaidyanathan, G. *Chem. Rev*. **1994**, *94*, 1999. (b) Vaidyanathan, G.; Herron, W. J.; Garvey, J. F. *J. Phys. Chem*. **1993**, *97*, 7880.
(29) Chang, H.-C.; Jiang, J.-C.; Hahndorf, I.; Lin, S. H.; Lee, Y. T.; Chang, H.-C. *J. Am. Chem. Soc*. **1999**, *121*, 4443.
(30) Herron, W. J.; Coolbaugh, M. T.; Vaidyanathan, G.; Garvey, J. F. *J. Am. Chem. Soc*. **1992**, *114*, 3684.
(31) Karpas, Z.; Eiceman, G. A.; Harden, C. S.; Ewing, P. B. W.; Smith, R. G. *Org. Mass Spectrom*. **1994**, *29*, 159.
(32) Karpas, Z.; Eiceman, G. A.; Ewing, R. G.; Harden, C. S. *J. Am. Soc. Mass Spectrom*. **1993**, *4*, 507.
(33) Vaidyanathan, G.; Garvey, J. F. *J. Phys. Chem*. **1994**, *98*, 2248.
(34) Lyktey, M. Y. M.; Rycroft, T.; Garvey, J. F. *J. Phys. Chem*. **1996**, *100*, 6427.
(35) Rexer, E. F.; DeLeon, R. L.; Garvey, J. F. *J. Chem. Phys*. **1997**, *107*, 4760.
(36) Campargue, R. *J. Phys. Chem*. **1984**, *88*, 4466.
(37) Feng, W. Y.; Lifshitz, C. *J. Phys. Chem*. **1994**, *98*, 6075.
(38) Shi, Z.; Wei, S.; Ford, J. V.; Castleman, A.W., Jr. *J. Chem. Phys*. **1992**, *200*, 142.
(39) Frisch, M. J.; Trucks, G. W.; Schlegel, H. B.; Gill, P. M. W.; Johnson, B. G.; Robb, M. A.; Cheesemna, G. R.; Keith, T.; Petersson, G. A.; Montgomery, J. A.; Raghavachari, K.; AlLaham, M. A.; Zakrzewski, V. G.; Ortiz, J. V.; Foresman, J. B.; Cioslowski, J.; Stefanov, B. B.; Nanayakkara, A.; Challacombe, M.; Peng, C. Y.; Ayala, P. Y.; Chen, W.; Wong, M. W.; Andres, J. L.; Replogle, E. S.; Gomperts, R.; Martin, R. L.; Fox, D.; Binkley, J. S.; DeFrees, D. J.; Baker, J.; Stewart, J. P.; Head-Gordon, M.; Gonzalez, C.; Pople, J. A. *Gaussian-94*; Gaussian, Inc.: Pittsburgh, PA, 1995.
(40) Weast, R. C., Ed. *CRC Handbook of Chemistry and Physics*; CRC Press: Cleveland, 1974.
(41) Wu, C.-C.; Jiang, J. C.; Boo, D. W.; Lin, S. H.; Lee, Y. T.; Chang, H.-C. *J. Chem. Phys*. **2000**, *112*, 176.
(42) Spartan Computational Chemistry Computer Program, Version 4.0, Wavefunction, Inc., 18401 Von Karman, Suite 370, Irvine, CA 92715.